

Design of PLL Controller for Resonant Frequency Tracking of Five-Level Inverter Used for Induction Heating Applications

Aws H. Al-Jrew*^{1,2}, Jawad R. Mahmood¹, Ramzy S. Ali¹¹Electrical Engineering Department, University of Basrah, Basrah, Iraq²Electronic and Communications Engineering Department, Al Muthanna University, Muthanna, Iraq

Correspondance

*Aws H. Al-Jrew

Electronic and Communications Engineering Department,
Al Muthanna University, Muthanna, Iraq

Email: aws.hashim@mu.edu.iq

Abstract

In this work, the phase lock loop PLL-based controller has been adopted for tracking the resonant frequency to achieve maximum power transfer between the power source and the resonant load. The soft switching approach has been obtained to reduce switching losses and improve the overall efficiency of the induction heating system. The jury's stability test has been used to evaluate the system's stability. In this article, a multilevel inverter has been used with a series resonant load for an induction heating system to clarify the effectiveness of using it over the conventional full-bridge inverter used for induction heating purposes. Reduced switches five-level inverter has been implemented to minimize switching losses, the number of drive circuits, and the control circuit's complexity. A comparison has been made between the conventional induction heating system with full bridge inverter and the induction heating system with five level inverter in terms of overall efficiency and total harmonic distortion THD. MATLAB/ SIMULINK has been used for modeling and analysis. The mathematical analysis associated with simulation results shows that the proposed topology and control system performs well.

Keywords

Induction Heating (IH), Phase Lock Loop (PLL), Resonant Series Inverter, Zero Voltage Switching (ZVS)..

I. INTRODUCTION

Induction heating is a technology used for heating metals or any conductive materials. It is used especially in industrial operations such as surface hardening, welding, tempering, brazing, and some home appliances like induction stoves or induction water heaters [1].

Induction heaters have become popular due to their fast heating durations, ability to heat a specific area, environmentally friendly, more efficient, safe, and saving energy [2, 3].

The power source designed for induction heating should be cost-effective and work better, so many studies have been conducted to improve the power semiconductor switching devices and microprocessors [4]. Many previous works used

classical topologies such as half-bridge and full-bridge inverters as a power supply for the induction heating system [5–8]. The use of classical topologies for inverters in medium voltage applications with two or four switches will increase the stress on switches, and then increased the losses as well [9]. From this point, the need to use a multilevel inverter in such high frequency application is required. The use of reduced switches multilevel inverter will reduce the complexity of driver circuit then cost saving [10].

Because of resonant condition reached in such induction heating system, these types of inverters with high switching frequency can be categorized as resonant inverters. The most common topologies for high-frequency resonant power con-

This is an open-access article under the terms of the Creative Commons Attribution License, which permits use, distribution, and reproduction in any medium, provided the original work is properly cited.
©2023 The Authors.

Published by Iraqi Journal for Electrical and Electronic Engineering | College of Engineering, University of Basrah.



version are current fed and voltage fed converters. The voltage fed resonant inverter has been used in the designed system because voltage source inverter VSI drives outperform current source inverter CSI drives in terms of efficiency. This is because we employ Insulated Gate Bipolar Transistor IGBT switching devices in VSI drives, which are more efficient than the Gate Turn Off Thyristor GTO or Symmetrical Gate Commutated Thyristor SGCT devices used in CSI versions. Another advantage of VSI over CSI, is that the VSI has a small size and its output voltage waveform does not depend on the type of load.

Induction heating system needed two principles to be in the designer consideration, first one is keeping the inverter in a resonant functioning state during the heating process, the control circuit must be able to track frequency automatically with the load variations [11–13]. This control circuit must respond faster and more accurate while increasing the output frequency of the inverter [14]. The second principle is achieving the soft switching conditions, the output voltage and inverter current must be in phase to avoid switching losses.

There is two control methods commonly used for these purposes, self-oscillating drivers and phase locked loop (PLL) [15]. The PLL has been utilized in this paper for induction heating system because it is more reliable and accurate specially when implemented and analyzed with a software based PLL algorithm. Many studies and research work used these control methods for induction heating applications [16–19].

M. Ali, R. Srinivasu, and T. R. Jyothsna [20], conducted a series resonant half-bridge inverter with a series parallel connection of capacitors for an induction heating system. They used PLL control unit to keep a unity power factor regardless to load changes. The performance of IH system with power rated of 6kW had been tested on frequency (50-150 kHz). They ignored the impact of overlap period and snubber components to get an information about the inverter output currents and voltages.

M. Roy and M. Sengupta [21], proposed 2kW, IH system with 10 kHz resonant frequency. They used digital-PLL based on FPGA to track the resonant frequency. The IH system consisted of CSI-fed IH coil linked to an H-bridge of four IGBTs with series diodes. At resonance state, the phase shift between voltage and current is ideally zero. The track of resonant frequency had been achieved by adjusting the switching frequency until the phase-shift is zero.

A. Namadmalan and J. S. Moghani [22], presented IH system with a mechanism for adjustable self-oscillating switching in current source parallel resonant inverters. To validate the performance of that tuning system, a IH system consisted of general-purpose (full bridge) CSI inverter with an operating frequency of 25-100 kHz had been used. A comparison had been done between the conventional technologies such as

phase-locked loop (PLL) with the self oscillating method , the latest methodology resulted in reduced voltage stress in the inverter. The used switching approach tracked the changing of resonance frequency. The self-oscillating switching method offered the capability to tune the phase error, where the phase error was important for parallel operating and zone control IH systems.

G. D. Goranov, N. D. Madzharov, and I. O. Kandov [23], worked on 20 kW IH system with a full bridge bipolar power supply inverter. Digital PLL control method had been conducted. They used digital format for the input and output parameters to get an easy adjustment during the heating process in dynamic mode. The sophisticated programming logic device called (coolrunner2 XILINX) had used for this purpose.

P. Herasymenko et al. [24], introduced control method for IH application included a software phase-locked loop for 10 kW IH system with a resonant voltage source power supply inverter. The software PLL control used to adjust the dead time between the inverter switches devices and regulate the fluctuation of load current amplitude and produced a phase shift between inverter output voltage and current.

H. Özbay, A. Karafil, and S. Öncü, in [25] discussed 250 W IH system with a sliding mode controlled PLL using a series resonant full bridge inverter. PLLs were utilized in IH applications to obtain zero voltage and zero current switching mode. Sliding mode control used with PLL to avoid the slow frequency tracking and make the controlling more reliable. Pulse density modulation PDM control method was improved to make the inverter operated at the resonant frequency because of significant decreasing in switching losses and electromagnetic noise . The operating frequency of the IH system range between (35-42 kHz).

P. Herasymenko [26], developed a 2.5 kW IH system of series resonant full bridge inverter with a digital control system based on STM32 and a software PLL controller. The used PLL system lead to phase synchronization between the output voltage and current of the series resonant inverter. The experimental studies done in that research work used the software PLL with several control methods, including phase shift control, pulse-density modulation control, and PS-PDM control. The range of frequencies used to test the system between (25 to 50 kHz). They claimed that the used PLL STM32-based system in that research was appropriate for induction heating application with simultaneously dual-frequency output current produced from two inverters.

The next section will take an overview about the conducted five level power supply inverter topology for this induction heating application. Section III discuss the PWM technique used for multilevel inverter. Section IV includes the description of the mathematical model used to design the PLL control unit. Section V, details a description of the block

diagram for the overall control system components. While section VI include the MATLAB simulation and modeling of the system. Finally, section VII include the conclusion from this work.

II. FIVE-LEVEL POWER SUPPLY INVERTER TOPOLOGY

A multilevel inverter (MLI) is an electronic power supply converter that produces multiple voltage levels. It is employed in applications with medium and high voltages [27, 28]. Multilevel inverters are important because of their power quality, harmonic amplitude reduction, and ability to provide an output voltage that is as close to a sinewave as possible. Multilevel resonant inverter topologies have experienced a substantial expansion in industrial applications in recent years due to the capability to deliver a voltage waveform of outstanding quality and reduce the current and voltage ratings of the power switches [29].

A reduced switches five-levels resonant inverter had been utilized as a power supply inverter for induction heating system. The configuration of the series resonant multilevel inverter explained with detailed in [30].

The general layout of the conducted power supply inverter for the induction heating system (reduced switches 5-level inverter) consists of two classical parts: the cascade H bridge MLI and the neutral point clamped MLI. The proposed topology of 5-level power supply inverter circuit diagram is shown in Fig. 1

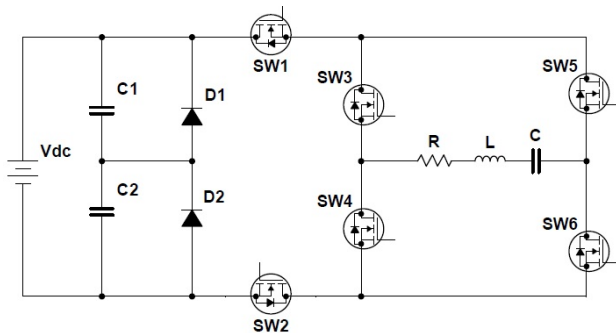


Fig. 1. Five Level Inverter Power Supply Model

As it clear in Figure (1), the inverter consists of six MOSFETs switching devices and two power diodes D1 and D2. The input DC voltage source is divided by connecting two identical capacitors C1 and C2 across the source. The split voltage is delivered to the H-bridge through two MOSFET switches SW1 and SW2 and two power diodes D1 and D2. The five operation modes are clarified in Fig. 2

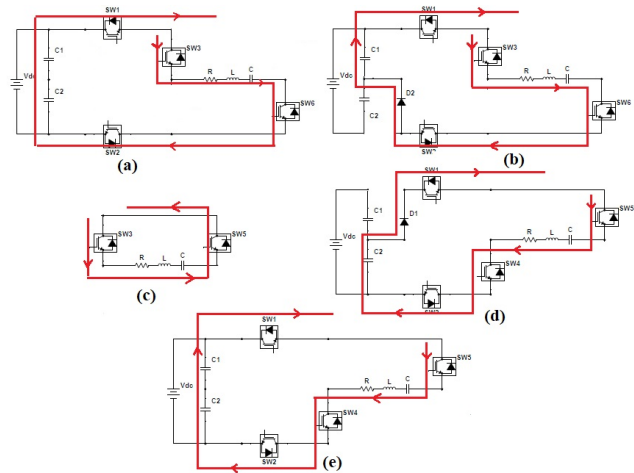


Fig. 2. Switching modes of five level power supply inverter (a) $V_o = +V_{dc}$ (b) $V_o = +0.5V_{dc}$ (c) $V_o = 0$ (d) $V_o = -0.5V_{dc}$ (e) $V_o = -V_{dc}$

III. PWM FOR THE USED POWER SUPPLY INVERTER

The multicarrier PWM techniques have been used in this study. These techniques have two categories phase shift and level shift. All carrier waves used in the multicarrier modulation technique known as phase shift modulation have a phase shift from one carrier to another. The number of carriers is associated with the number of voltage levels. The same frequency and peak-to-peak amplitude should be used for all carriers.

The relationship between voltage levels and the number of carriers in the level shift PWM technique is similar to that of phase shift. The difference between level shift and phase shift can be noticed in the disposition of the triangular carrier. The phase shift and the level shift multicarrier PWM techniques have a similar relationship between the levels of voltage and carrier number. The level shift PWM approach for the employed five level inverter was the subject of this work.

IV. THE MATHEMATICAL MODEL DESCRIPTION

The adopted mathematical model described with details in [1] has been used to build the modified control system for a five level series resonant inverter in the next section. The phase angle between the inverter voltage v_{inv} and capacitor voltage v_c has been adjusted to achieve the PLL concept. The phase difference error between the inverter and capacitor voltages is described as:

$$e(k) = x_f(k) - \frac{1}{2} \quad (1)$$

Where x_f DC average voltage.

If the system operates in a steady-state, the DC voltage x_f can be expressed as follow:

$$x_{fss} = \frac{\varphi}{\pi} = u_f \quad (2)$$

Where u_f : the low pass filter input's average value, and φ : the phase difference.

In the transient operation, the relationship between x_f and u_f can be expressed as :

$$\frac{dx_f}{dt} = -\left(\frac{1}{\tau_f}\right)x_f + \left(\frac{1}{\tau_f}\right)u_f \quad (3)$$

Where τ_f is the filter time constant which is $\tau_f = RC$. For the resonant load of inverter operating in the steady state conditions, the relation between phase difference φ and switching period T can be given as:

$$\varphi(T) = \tan^{-1}\left(\frac{R_f C_s \frac{2\pi}{T}}{1 - \left(\frac{2\pi}{\omega_o T}\right)^2}\right) \quad (4)$$

During transient operations in which the period T fluctuates slowly, it is presumed that the equation above is approximately correct. Furthermore, Equation "(4)," is achieved by assuming a purely sinusoidal inverter output voltage. The following is a discretization of "(3),":

$$x_f(k+1) = ax_f(k) + b \frac{\varphi(T(k))}{\pi} \quad (5)$$

Where $a = e^{-\frac{T_s}{\tau_f}}$, $b = (1-a)$

During the heating process, the induction heating system detunes and the relation between the next resonance periodical time $T(k+1)$ and the previous one $T(k)$ can be expressed as follows:

$$T(k+1) = T(k) + K_c e(k+1) \quad (6)$$

Where K_c is the integral gain. The closed-loop equation can be expressed as:

$$T(k+1) = T(k) + K_c \left(ax_f(k) + b \frac{\varphi(T(k))}{\pi} - \frac{1}{2} \right) \quad (7)$$

The jury test of stability used for discrete systems is a simple form of the Routh-Hurwitz algorithm which checks if the polynomial roots are enclosed by the unit circle. The

range of integral stability gain K_c can be determined using this Jury's test as follow:

$$0 < K_c < \left(\frac{1+a}{1-a}\right) 2\pi^2 RC \quad (8)$$

PLL circuits keep tracking the resonance frequency automatically to maintain soft-switching under varying load conditions. The zero phase difference between the input current and output voltage must be obtained in resonance state to achieve zero voltage switching ZVS.

Zero voltage switching ZVS approach is utilized to reduce switching losses and enhance the system efficiency, which is commonly used with resonant inverter. ZVS can be accompanied with PLL controller to obtain the resonant frequency tracking. The tank circuit's resonance behavior and the frequency feedback from the PLL controller are taken into consideration by the ZVS control when determining the best time to switch the power transistors.

The capacitor voltage v_c and the inverter voltage v_{inv} transform to square waves using Zero crossing detector ZCD. Then the output of ZCD is applied to an XOR gate and the output of this gate is filtered to get a DC voltage x_f which is proportional to the phase difference between the inverter and capacitor voltages as illustrated in Fig. 3.

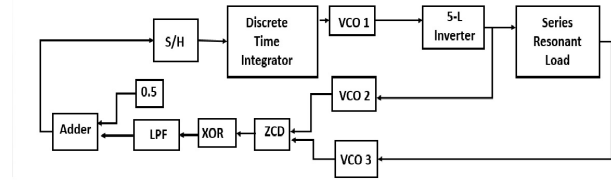


Fig. 3. The Structure of the PLL Based Control Circuit

The switching frequency is adjusted after comparison between the average DC voltage (x_f) and a value of 90 degrees, to make the phase difference zero. When this requirement is fulfilled, the voltage and current of the inverter are assured to be in phase.

V. DESCRIPTION OF THE CONTROL SYSTEM

The structure of the PLL based modified control circuit is shown in Fig. 3 as an example of how it works. The system block diagram consists of the following parts: Zero Crossing Detector ZCD which is responsible for detecting the variation from positive to negative level of the sinusoidal voltage waveforms. Exclusive OR gate, where the output from this logic

gate will compare with reference value of the duty cycle. Low Pass Filter LPF, adder, sample-and-hold unit (S/H) used to sample the error, and this operation represents (analog to digital) conversion. Discrete-time integrator represents the integral controller, and the last part of control unit is the Voltage Control Oscillator VCO where the VCO output represents output signal of PLL control unit. In the modeling of the control system using MATLAB, the PLL controller can be simplified by removing the LPF stage as shown in the next section which can be compensated with software algorithms instead of analog one. The other modification on the PLL controller is the use of VCO output-generated signal as a reference signal for PWM issue.

The inverter output voltage v_{inv} and the capacitor resonant voltage v_c are measured then applied to Zero Crossing Detector ZCD. The outputs from ZCD are compared in an XOR logic gate then applied to low pass filter LPF. The phase difference error between the inverter and capacitor voltages discretized to $e(k)$. The discrete-time integrator produces a new resonance periodical time $T(k + 1)$, and new drive pulses of the MOSFET will be created using a VCO. As a result, the inverter can now operate in the new resonant state and track the new resonance frequency.

VI. SIMULATION AND MODELING OF SYSTEM

The SIMULINK model of IH system with the PLL control circuit for the five levels inverter power supply is illustrated in Fig. 4 The parameters used in this model is $R=26.6\Omega$, $L=120\mu\text{H}$, $C=0.08\mu\text{F}$, sampling time $1\mu\text{s}$, initial resonant frequency of the inverter $f_o=51.367\text{ kHz}$, the applied DC voltage source is 48 v. The value used for the K_c has been calculated according to the “(8)”. The stability of the system obtained when the value of integral gain K_c between 0 and 40×10^{-6} .

The PWM signals introduced in Figure (4c) P1, P2, N1,N2 and PNO has been illustrated in Fig. 5. The six gates signals are shown in Fig.6:

The PLL output signal is illustrated in Fig. 7 which is close to the sinusoidal waveform and this signal works as modulating signal in PWM. The phase angle difference between inverter voltage v_{inv} and capacitor voltage v_c waveforms is $\pi/2$ as shown in Fig. 8 and this difference changes after the system detunes from resonant frequency.

The output waveform of XOR gate has 50% duty cycle when the system in resonance state at resonant frequency 51.3 kHz as illustrated in Figure (9a), but it will vary if the system detunes from resonant state as illustrated in Figure (9b) when the system operate at frequency 40kHz which is below the resonant frequency. The duty cycle of XOR gate will also detune if we choose frequency above the resonant. As a result, the XOR output waveform in this PLL system

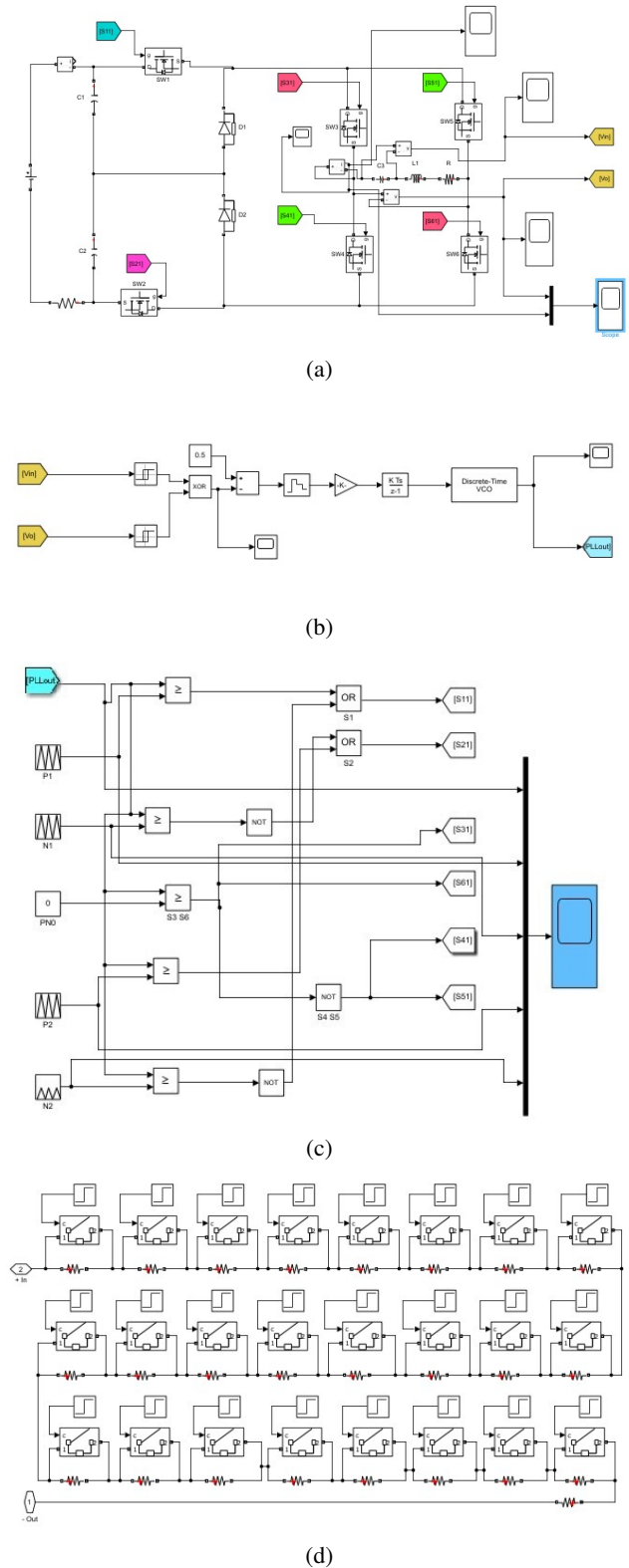


Fig. 4. PLL Base Control Simulation Model of IH System (a) Overall IH Circuit Model (b) PLL Control Unit (c) PWM Logic Circuit of Gate Signals (d) Variable Workpiece Resistance

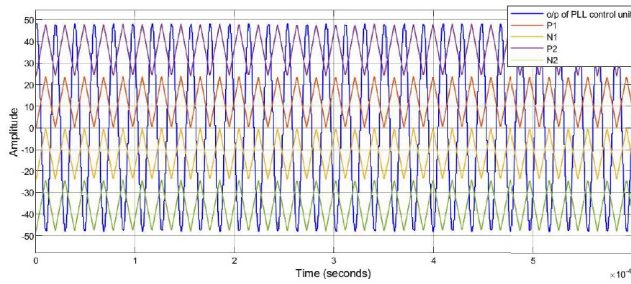


Fig. 5. PWM Signals

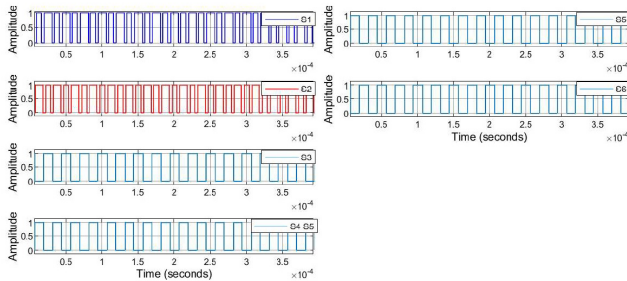


Fig. 6. Inverter Gate Signals

can be considered as a criteria used to determine whether the system in resonant state or not.

Fig. 10 illustrates the inverter output voltage waveform.

The IH system has been tested under variable workpiece resistance as shown in Fig. 11.

Figure 12 represents the inverter load current waveform under variable resistance for the workpiece. Fig. 13 represents the capacitor voltage waveform under variable resistance for the workpiece, which is a purely sinusoidal voltage waveform. The phase angles between voltage and current are the same, and their simulation waveforms match the theory analysis we discussed before

The load loop current and voltage waveforms at frequency below the resonant frequency (40 KHz) is shown in Figure (14) 14 where the system still detunes before reaching the resonance state, the Zero Voltage Switching ZVS approach fail to take place and there is phase difference between the output voltage and inverter current.

In Fig. 15, the load current and voltage reach the resonance state at the frequency 51.3KHz where the output voltage and inverter current are in phase and the soft switching is obtained. As a result, the system operates at the resonance frequency.

A comparison has been made between the proposed PLL-based IH system with a multilevel inverter used in this article and the IH system with a PLL controller using a full bridge inverter. The comparison has been made in terms of total

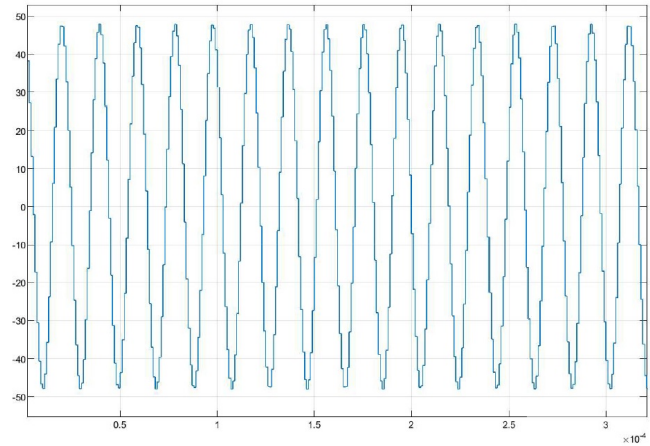


Fig. 7. PLL Output Signal

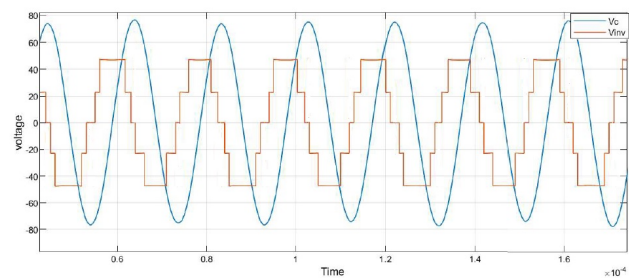


Fig. 8. Capacitor and Inverter Voltage Waveforms at Resonant Frequency 51.3 kHz

harmonic distortion THD, overall efficiency.

The conventional full bridge IH system with PLL controller shown in Fig. 16.

The total harmonic distortion THD results for the two topologies are shown in Fig. 17. It seems that the THD for the IH system with a five-level inverter is (28.88%) which is lower as compared with (49.46%) for the IH system with a full bridge inverter.

The total harmonic distortion THD for both systems also was tested with the simplified PLL controller without using LPF and the results were (29.49%), (and 49.37%) for five level and full bridge IH systems respectively.

The overall system efficiency for a conventional IH system with full bridge inverter is (98.48%) and it remains the same if we used the simplified PLL controller without LPF. On the other hand, the overall efficiency of IH system with reduced switches five level inverter is (89.48%) and it remains the same if we used the simplified PLL controller without LPF. Even though the overall efficiency for IH system with five level inverter is lower than the full bridge topology, which is normal due to the added driving circuit and wiring, but the

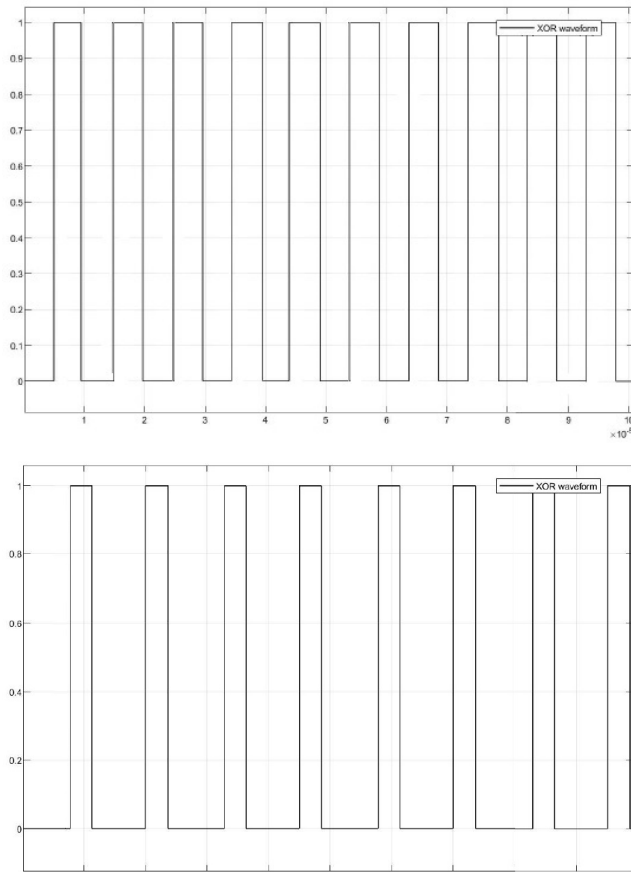


Fig. 9. The XOR Waveform (a) at resonance frequency 51.3 kHz (b) at a frequency below resonant frequency 40 kHz

effectiveness of using the simplified PLL controller is clear by not effect on the efficiency for both topologies. The simulation results obtained agree with the mathematical analysis obtained in section IV.

VII. CONCLUSION

In this paper, a PLL-based approach has been used to track the resonance frequency and also to achieve soft switching for the induction heating system. The adopted inverter power supply has been implemented with a reduced number of switches to get five-level inverter feeding the induction heating load. The reduced switching approach resulted in a reduction of the switching losses and also the number of drive circuits used. The MATLAB simulation of the developed mathematical model shows good results in terms of resonance frequency tracking and achievement of soft switching which has been obtained by checking up the phase variation between the load loop current and inverter output voltage waveform.

The work also included testing the system's stability. Ac-

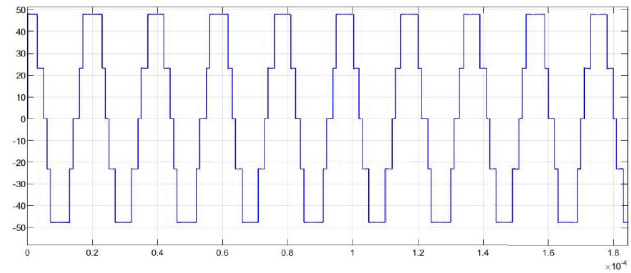


Fig. 10. Inverter Voltage Waveform

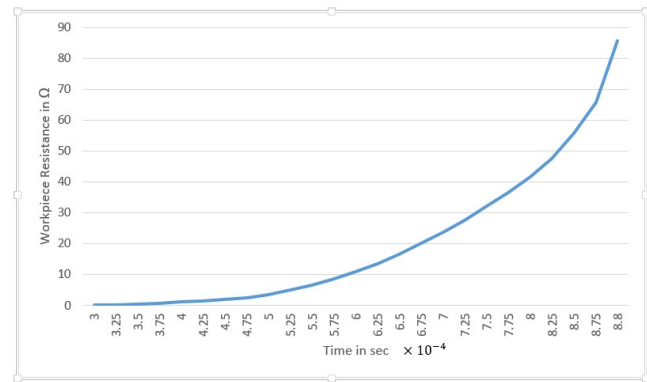


Fig. 11. Variable Workpiece Resistance for IH System

ording to Jury's Stability test, the system shows good stability level where the value of integral stability gain K_c lies between (0 to 40×10^{-6}).

The article also included a comparison made between two IH systems with a conventional full bridge inverter and a reduced switch five-level inverter. It shows that the reduced switch five-level IH system perform better than the full bridge in term of THD, while the overall efficiency of the full bridge is higher than the reduced switch five-level inverter with the IH system.

CONFLICT OF INTEREST

The authors have no conflict of relevant interest to this article.

REFERENCES

- [1] N. Bayndtr, O. Kukrer, and M. Y. Y, "Dsp-based pll-controlled 50-1 00 khz 20 kw high- frequency induction heating system for surface hardening and welding applications,," *IEE Proc-Electr. Power Appl.*, vol. 150 no.3, pp. 365–371, 2003.
- [2] Y. L. Cui, K. He, Z. W. Fan, and H. L. Fan, "Study on dsp-based pll-controlled superaudio induction heating power supply simulation,," in *2005 Int. Conf. Mach. Learn. Cybern.*, pp. 1082–1087, 2005.

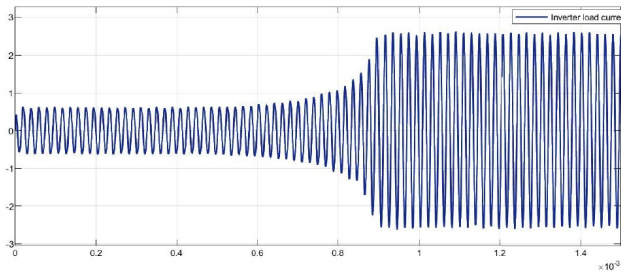


Fig. 12. Inverter Load Current with Variable Workpiece Resistance

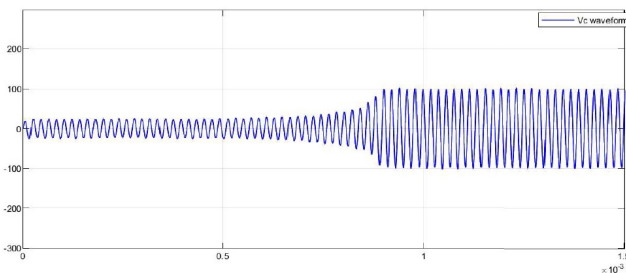


Fig. 13. Capacitor voltage waveform with variable workpiece resistance

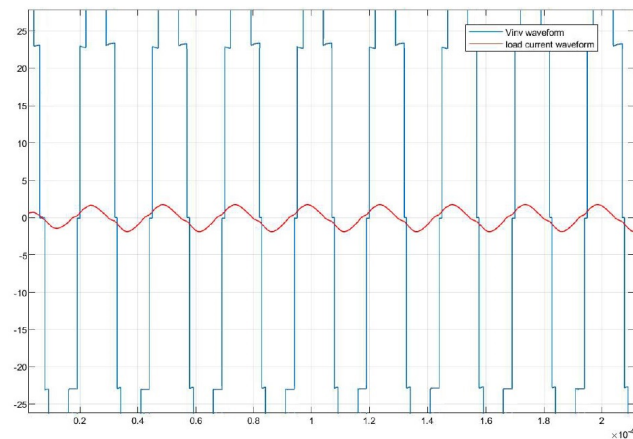
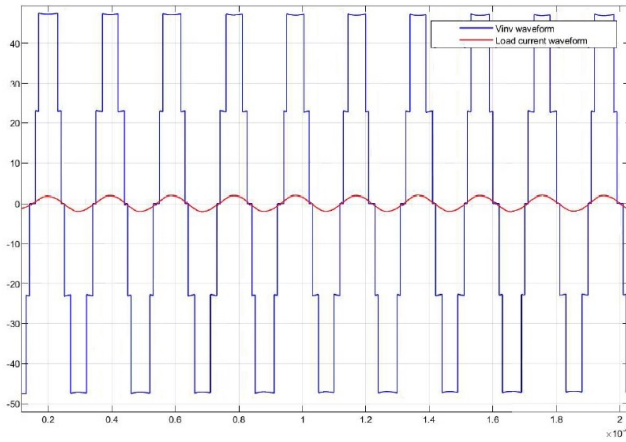
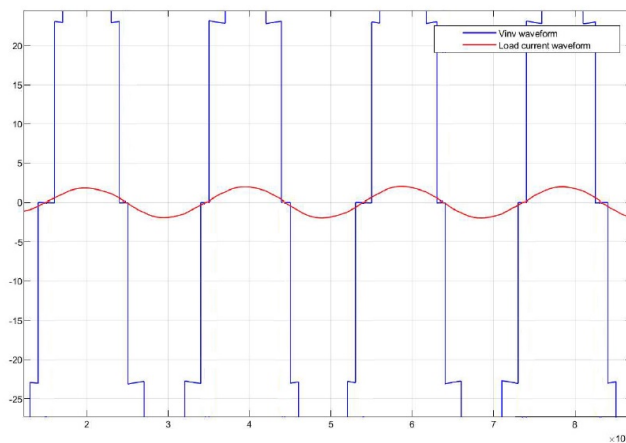


Fig. 14. Load Loop Current and Inverter Output Voltage Waveform Below Resonant Frequency 40 KHz

- [3] Y. Wang, Y. Li, Y. Peng, and X. Qi, "Research and design on igbt induction heating power supply," *Energy Procedia*, vol. 16, no. PART C, pp. 1957–1963, 2012.
- [4] S. Choi, C. Lee, I. Kim, J. H. Jung, and D. H. Seo, "New induction heating power supply for forging applications using igbt current-source pwm rectifier and inverter," *KIEE Electr. Mach. Energy Convers. Syst.*, pp. 709–713, 2018.
- [5] O. Lucia, J. M. Burdio, I. Millan, J. Acero, and D. Puyal, "Load-adaptive control algorithm of half-bridge series resonant inverter for domestic induction heating," *IEEE Trans. Ind. Electron.*, pp. 3106–3116, 2009.
- [6] Z. Waradzyn, A. Penczek, and A. Skala, "Analysis of the load current harmonics content in a series resonant inverter for induction heating controlled using various cases of the avc control strategy," in *Proc. 2018 Conf. Electrotechnol. Process. Model. Control Comput. Sci. EPMCCS 2018*, pp. 1–9, 2018.
- [7] J. Villa, A. Mur, J. I. Artigas, L. A. Barragan, I. Uriza, and D. Navarro, "Output voltage estimation of a half-bridge inverter for domestic induction heating applications," in *IECON Proc. (Industrial Electron. Conf.)*, pp. 5081–5086, 2019.
- [8] C. Hammouma and H. Zeroug, "Enhanced frequency adaptation approaches for series resonant inverter control under workpiece permeability effect for induction hardening applications," *Eng. Sci. Technol. an Int. J.*, vol. 27, pp. 1–13, 2022.
- [9] P. Omer, J. Kumar, and B. S. Surjan, "A review on reduced switch count multilevel inverter topologies," *IEEE Access*, vol. 8, pp. 22281–22302, 2020.
- [10] R. K. Kumawat and D. K. Palwalia, "A comprehensive analysis of reduced switch count multilevel inverter," *Aust. J. Electr. Electron. Eng.*, vol. 17, no. 1, pp. 13–27, 2019.
- [11] B. Nagarajan and R. R. Sathi, "Phase locked loop based pulse density modulation scheme for the power control of induction heating applications," *J. Power Electron.*, vol. 15, no. 1, pp. 65–77, 2015.
- [12] A. Cristina and O. A. Pop, "Method for detecting resonance frequency in induction heating systems," in *IEEE 25th Int. Symp. Des. Technol. Electron. Packag. IEEE Xplore, October*, pp. 295–298, 2019.
- [13] C. Hammouma, H. Zeroug, and A. Attab, "A new approach for adaptive frequency in series resonant inverter for induction hardening," in *3rd Int. Conf. Electr. Sci. Technol. Maghreb, Cist.*, pp. 1–6, 2018.
- [14] S. Oncu and H. Ozbay, "Simulink model of parallel resonant inverter with dsp based pll controller," *Elektron. ir Elektrotehnika*, vol. 21, no. 6, pp. 14–17, 2015.
- [15] M. H. Khazaal, I. M. Abdulbaqi, and R. H. Thejel, "Design, simulation and implementation of a self-oscillating



(a)



(b)

Fig. 15. Load Current and Inverter Output Voltage Waveform at Resonant Frequency 51.3KHz (a) Ten Cycles View (b) Four Cycles View

control circuit to drive series resonant inverter feeding a brazing induction furnace,” in *Al-Sadiq Int. Conf. Multi-discip. IT Commun. Tech. Sci. Appl. AIC-MITCSA 2016*, pp. 178–183, 2016.

- [16] A. Namadmalan and J. S. Moghani, “Self-oscillating switching technique for current source parallel resonant induction heating systems,” *Journal of Power Electronics*, vol. 12, no. 6, pp. 851–858, 2012.
- [17] A. Namadmalan, “Self-oscillating tuning loops for series resonant inductive power transfer systems,” *IEEE Trans. Power Electron.*, vol. 31, no. 10, pp. 7320–7327, 2016.

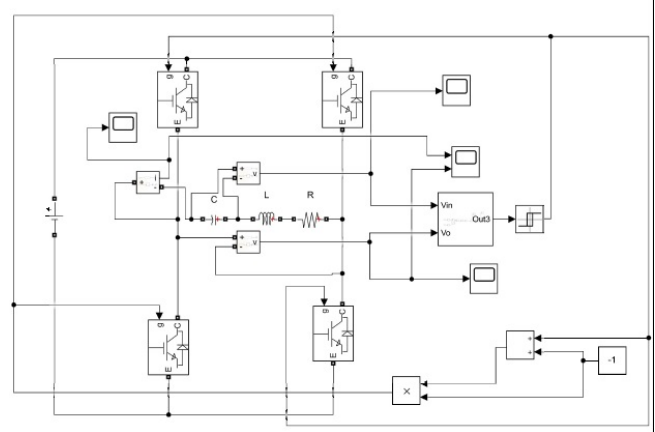
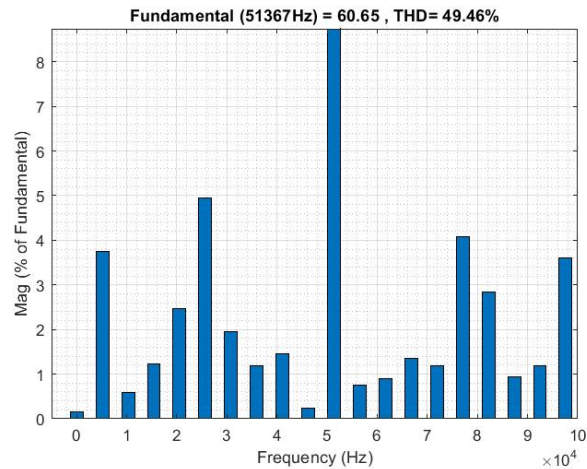
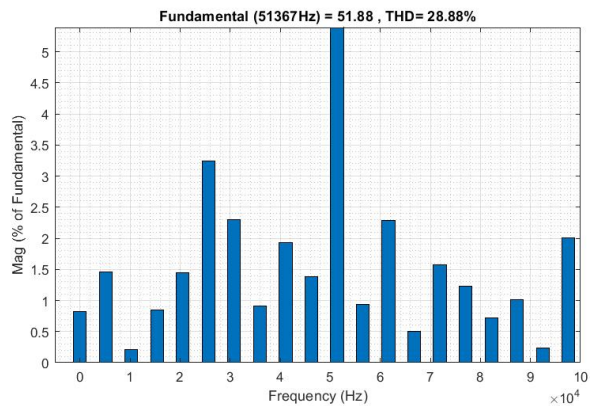


Fig. 16. IH Circuit Model With Full-Bridge Inverter

- [18] B. Meziane and H. Zeroug, “Improved efficiency determination for a pll-controlled series resonant inverter for induction metal surface hardening,” in *2015 IEEE Industry Applications Society Annual Meeting*, pp. 1–8, 2015.
- [19] S. K. Singh and A. Agarwal, “Modelling and controlling of induction heating unit for induction cooking application,” in *J. Phys. Conf. Ser.*, vol. 1478, pp. 1–10, 2020.
- [20] M. Ali, R. Srinivasu, and T. R. Jyothsna, “Phase locked loop control of 50-150 khz half bridge resonant type inverter for induction heating applications,” *Int. J. Eng. Res. Appl.*, vol. 4, no. 8, pp. 21–27, 2014.
- [21] M. Roy and M. Sengupta, “Application of fpga based pll in a csi fed induction heating prototype,” in *IEEE Int. Conf. Power Electron. Drives Energy Syst.*, pp. 1–4, 2014.
- [22] A. Namadmalan and J. S. Moghani, “Tunable self-oscillating switching technique for current source induction heating systems,” *IEEE Trans. Ind. Electron*, vol. 61, no. 5, pp. 2556–2563, 2014.
- [23] G. D. Goranov and N. D. Madzharov, “Resonant inverter with all digital pll control,” in *Int. Conf. Expo. Electr. Power Eng. EPE*, pp. 653–657, 2016.
- [24] P. Herasymenko, V. Hutsaliuk, V. Pavlovskiy, and O. Yurchenko, “A software phase-locked loop of control system of a series-resonant voltage-source inverter for induction heating equipment,” in *2017 IEEE 1st Ukr. Conf. Electr. Comput. Eng. UKRCON 2017 - Proc.*, pp. 384–389, 2017.
- [25] H. Ozbay, A. Karafil, and S. Oncu, “Sliding mode pll-dpm controller for induction heating system,” *Turkish J.*



(a)



(b)

Fig. 17. Total Harmonic Distortion THD Analysis for IH System With (a) Full Bridge Inverter (b) Reduced Switch Five Level Inverter

Electr. Eng. Comput. Sci., vol. 29, no. 2, pp. 1241–1258, 2021.

- [26] P. Herasymenko, “Inexpensive high-performance stm32-based software pll for series-resonant inverters in induction heating equipment,” in *12th Int. Symp. Adv. Top. Electr. Eng. Bucharest, Rom.*, pp. 1–6, 2021.
- [27] D. Prasad, C. Dhanamjayulu, S. Padmanaban, J. B. Holm-Nielsen, F. Blaabjerg, and S. R. Khasim, “Design and implementation of 31-level asymmetrical inverter with reduced components,” *IEEE Access*, vol. 9, pp. 22788–22803, 2021.
- [28] A. AbdAli, A. Abdulabbas, and H. Nekad, “Nonconventional diode clamped multilevel inverter with reduced

number of switches,” *Iraqi J. Electr. Electron. Eng.*, vol. 16, no. 2, pp. 1–12, 2020.

- [29] A. E. T. Maamar, M. Helaimi, R. Taleb, M. Kermadi, S. Mekhilef, A. Wahyudie, and M. Rawa, “Analysis and small signal modeling of five-level series resonant inverter,” *IEEE Access*, vol. 9, pp. 109384–109395, 2021.
- [30] A. H. Al-jrew, J. R. Mahmood, and R. S. Ali, “Comparison of new multilevel inverter topology with conventional topologies used for induction heating system,” *Iraqi J. Electr. Electron. Eng.*, vol. 18, no. 1, pp. 48–57, 2022.